EJN European Journal of Neuroscience FENS Federation of European Neuroscience Societies

European Journal of Neuroscience, Vol. 44, pp. 1734–1746, 2016 doi:10.1111/ejn.13271

MOLECULAR AND SYNAPTIC MECHANISMS

Impact of neural cell adhesion molecule deletion on regeneration after mouse spinal cord injury

Vedangana Saini,[1,2] Gabriele Loers,[1] Gurcharan Kaur,[2] Melitta Schachner[1,3,4,*] and Igor Jakovcevski[5,6,*]
[1]Zentrum für Molekulare Neurobiologie, Universitätskrankenhaus Hamburg-Eppendorf, Universität Hamburg, Hamburg, Germany
[2]Department of Biotechnology, Guru Nanak Dev University, Punjab, India
[3]Center for Neuroscience, Shantou University Medical College, 22 Xin Ling Road, Shantou 515041, China
[4]Keck Center for Collaborative Neuroscience and Department of Cell Biology and Neuroscience, Rutgers University, Piscataway, NJ 08854, USA
[5]Institute for Molecular and Behavioral Neuroscience, University Hospital Cologne, Köln, Germany
[6]Experimental Neurophysiology, German Center for Neurodegenerative Diseases, Ludwig-Erhard-Allee 2, D-53175 Bonn, Germany

Keywords: astrocyte, cholinergic system, locomotor recovery, microglia, monoaminergic system

Edited by Deniz Kirik
Received 23 June 2015, revised 28 April 2016, accepted 9 May 2016

Abstract

The neural cell adhesion molecule (NCAM) plays important functional roles in development of the nervous system. We investigated the influence of a constitutive ablation of NCAM on the outcome of spinal cord injury. Transgenic mice lacking NCAM (NCAM−/−) were subjected to severe compression injury of the lower thoracic spinal cord using wild-type (NCAM+/+) littermates as controls. According to the single-frame motion analysis, the NCAM−/− mice showed reduced locomotor recovery in comparison to control mice at 3 and 6 weeks after injury, indicating an overall positive impact of NCAM on recovery after injury. Also the Basso Mouse Scale score was lower in NCAM−/− mice at 3 weeks after injury, whereas at 6 weeks after injury the difference between genotypes was not statistically significant. Worse locomotor function was associated with decreased monoaminergic and cholinergic innervation of the spinal cord caudal to the injury site and decreased axonal regrowth/sprouting at the site of injury. Astrocytic scar formation at the injury site, as assessed by immunohistology for glial fibrillary acidic protein at and around the lesion site was increased in NCAM−/− compared with NCAM+/+ mice. Migration of cultured monolayer astrocytes from NCAM−/− mice was reduced as assayed by scratch wounding. Numbers of Iba-1 immunopositive microglia were not different between genotypes. We conclude that constitutive NCAM deletion in young adult mice reduces recovery after spinal cord injury, validating the hypothesized beneficial role of this molecule in recovery after injury.

Introduction

Spinal cord injury causes severe deficits, often associated with permanent disability. Various therapeutic strategies aimed at decreasing the activities of inhibitory molecules and at promoting neuronal survival and axonal re-growth have led to some success (Silver & Miller, 2004; Karimi-Abdolrezaee & Billakanti, 2012). Recognition molecules play important roles in these phenomena and underlie formation of neural circuits not only during neural development, but also in the adult, when synaptic activities change and recovery from injury is required (Schachner, 1997; Loers & Schachner, 2007; Maness & Schachner, 2007).

One such cell adhesion molecule, which plays a key role in cell migration and plasticity changes in the developing and adult nervous system, is the neural cell adhesion molecule (NCAM) (Kiss *et al.*, 2001). NCAM interacts with other cell adhesion molecules (Kadmon *et al.*, 1990; Kristiansen *et al.*, 1999), including extracellular matrix components (Takei *et al.*, 1999; Kiss *et al.*, 2001). It carries the carbohydrate polysialic acid (PSA) as a post-translational modification, leading to distinct properties of the polysialylated vs. non-polysialylated protein backbone, which distinguishes it from several other neural adhesion molecules. The polysialylated form of NCAM, previously known as embryonic form of NCAM (Finne *et al.*, 1983) promotes synaptic plasticity (Kiss *et al.*, 2001; Rutishauser, 2008; Senkov *et al.*, 2012), dynamic neuron-glia associations in the hypothalamus (Kumar *et al.*, 2012) and spatial learning and memory (Senkov *et al.*, 2006; Maness & Schachner, 2007; Rutishauser,

---

Correspondence: Igor Jakovcevski, [6]Experimental Neurophysiology, as above.
E-mail: igor.jakovcevski@dzne.de
and
Melitta Schachner, [3]Center for Neuroscience or [4]Keck Center for Collaborative Neuroscience and Department of Cell Biology and Neuroscience, as above.
E-mails: schachner@stu.edu.cn; schachner@dls.rutgers.edu

*These authors contributed equally to this work.

2008). NCAM also facilitates guidance of corticospinal axons during rat brain development (Joosten & Bär, 1999) and growth cone protrusion from cultured chick dorsal root ganglion neurons (Takei *et al.*, 1999).

Several lines of evidence suggest the importance of NCAM in regeneration after traumatic injury in the nervous system. A transient increase in the expression of PSA-NCAM is observed in neurons and astrocytes in the vicinity of the lesion site of the adult rat spinal cord (Bonfanti *et al.*, 1996). NCAM is also expressed by meningeal cells in the pia mater and Schwann cells in spinal nerve roots during cellular re-organization after spinal cord hemisection (Brook *et al.*, 2000). Its expression is reported to be upregulated in dorsal fiber tracts after complete spinal cord transection (Tzeng *et al.*, 2001). Lentivirus-induced expression of polysialylated NCAM at the site of spinal cord injury (Zhang *et al.*, 2007) or grafts of PSA-NCAM over-expressing Schwann cells lead to enhanced functional recovery (Papastefanaki *et al.*, 2007; Ghosh *et al.*, 2012).

Using an experimental paradigm similar to ours Zhang *et al.* (2010) demonstrated that NCAM promotes axogenesis and locomotor recovery after spinal cord contusion injury in mice. On the basis of these observations, we studied several molecular mechanisms underlying NCAM's role in regulating the extent of synaptic inputs to motoneurons, in particular to motoneurons caudal to the lesion site, and the histological disposition of the injury site itself by comparing mice constitutively deficient in NCAM with their wild-type littermates. Results indicate that NCAM is beneficial for locomotor recovery, reduces astrocytic scarring and predisposes for synaptic rearrangements following injury. Because our results indicating reduced astrocytic scarring *in vivo* were incongruent with the previous report (Zhang *et al.*, 2010), we additionally tested the effects of the ablation and addition of NCAM on the migration of cultured astrocytes.

Materials and methods

Animals

Three-month-old NCAM−/− female mice and their NCAM+/+ female littermates (Cremer *et al.*, 1994) from heterozygous breeders were maintained at the specific pathogen-free animal facility of the Center for Neurobiology Hamburg and used for spinal cord injury. For cell culture experiments 1-day-old NCAM−/− and NCAM+/+ mice or C57BL6/J mice of either sex were used. Genotyping was performed by the allele-specific polymerase chain reaction from the tail cut samples as described (Cremer *et al.*, 1994). Mice were kept at standard laboratory conditions with food and water supply *ad libitum* and with an artificial 12 h light/dark cycle. All experiments were conducted in accordance with the German and European Community laws on protection of experimental animals, and the procedures used were approved by the responsible committee of The State of Hamburg (permit number G09/098). Numbers of animals studied in the different experimental groups are indicated in the figure legends. All experiments, data acquisition and analyses were performed by researchers blinded to genotype/treatment.

Antibodies and reagents

The following antibodies were used: goat anti-choline acetyltransferase (ChAT, Chemicon, Hofheim, Germany; 1 : 100), rabbit anti-tyrosine hydroxylase (TH, Chemicon, 1 : 800), mouse anti-glial fibrillary acidic protein (GFAP, Sigma-Aldrich, 1 : 1000), rabbit anti-ionized calcium binding adaptor molecule 1 (Iba-1, Sigma-Aldrich, 1 : 1500), rabbit anti-neurofilament 200 (NF-200, Sigma/Aldrich, 1 : 1000), mouse anti- glyceraldehyde-3-phosphate dehydrogenase (GAPDH, Sigma-Aldrich, 1 : 1000) rabbit anti-vesicular glutamate transporter 1 (VGluT1, Synaptic Systems, Göttingen, Germany, 1 : 1000), rabbit anti-vesicular inhibitory neurotransmitter transporter (VGAT, Synaptic Systems, 1 : 1000) and rabbit anti-Ki67 (Abcam, Cambridge, UK; 1 : 500). The Cy-3- or Cy-2- conjugated secondary antibodies used for indirect immunofluorescence were as follows: goat anti-rabbit, goat anti-mouse and donkey anti-goat (Dianova, Hamburg, Germany). The following reagents were used: Dulbecco's modified Eagle's medium (DMEM), penicillin/streptomycin, fetal calf serum (Life Technologies); Fc from human IgG (Dianova); NCAM-Fc was prepared as described (Chen *et al.*, 1999); endoglycosidase N (EndoN) and mouse monoclonal antibody 735 against PSA were kind gifts from Dr. Rita Gerardy-Schahn at the Zentrum Biochemie, Zelluläre Chemie, Medizinische Hochschule, Hannover, Germany.

Surgical procedures

All surgical procedures were performed as described (Mehanna *et al.*, 2010). In brief, mice were anesthetized by intraperitoneal injections of ketamine and xylazine (100 mg/kg Ketanest®, Parke-Davis/Pfizer, Karlsruhe, Germany; 16 mg/kg Rompun®, Bayer, Leverkusen, Germany). Intraoperative analgesia was achieved by subcutaneous injection of buprenorphine (1 mg/kg, Temgesic®, Merck, Darmstadt, Germany). Laminectomy was performed at the T7-T9 level, corresponding to spinal cord segments T10-11, with mouse laminectomy forceps (Fine Science Tools, Heidelberg, Germany) after careful removal of dorsal and lateral vertebral laminae. A mouse spinal cord compression device was used to elicit compression injury at the level of spinal cord segments T10-11 (Curtis *et al.*, 1993). Compression force (degree of closure of the forceps) and duration were controlled by an electromagnetic device. The spinal cord was maximally compressed (100%, according to the operational definition of Curtis *et al.* (1993)) for 1 s by a time-controlled current flow through the electromagnetic device, using maximum current (12 V). The skin was then surgically closed using 6-0 nylon stitches (Ethicon, Norderstedt, Germany). After surgery, mice were kept on a heated mat (35 °C) for several hours to prevent hypothermia and thereafter singly housed in a temperature-controlled (22 °C) room with water and standard food provided *ad libitum*. During the post-operative time period the bladders of the animals were manually voided twice daily, and the animals received the non-steroidal anti-inflammatory drug carprofen (5 mg/kg Rimadyl®, Pfizer).

Analysis of motor function

All tests of motor function were performed during the light phase of the light/dark cycle in a moderately lit (approximately 200 lux) custom made acrylic glass arena 60 × 60 cm in size. The recovery of ground locomotion was evaluated using the Basso Mouse Scale (BMS) score (Basso *et al.*, 2006) and a single-frame motion analysis (Apostolova *et al.*, 2006). The latter method included evaluation of two parameters in the beam-walking test: foot-stepping angle and rump-height index. Mice performing these tests were video recorded from the lateral aspect, allowing objective quantitative analysis. The foot-stepping angle is defined by a line parallel to the dorsal surface of the hindpaw and the horizontal line of the beam. The angle is measured at the beginning of the stance phase on each leg. In intact mice, this phase is well defined and the angle is around 25°. After spinal cord injury and severe loss of locomotor abilities, mice drag behind their hindlimbs with the dorsal paw surface facing the beam. The angle is increased to > 160°. If the foot-stepping angle is lower than 90° it is characteristic of plantar stepping, whereas angles > than 90° indicate dorsal paw placing. The second parameter, the rump-height index, was estimated from the same recordings used for measurements of the foot-stepping angle. The parameter is defined as the vertical distance from the animal's tail base to the beam, normalized to the thickness of the beam measured along the same vertical line. Assessment of all parameters was performed before and at 1, 3 and 6 weeks after the injury. Values for the left and right extremities were averaged. The recovery index was calculated for each measured parameter on an individual animal basis according to a published formula (Apostolova *et al.*, 2006), which estimates regain of function as a fraction of the functional loss induced by injury, expressed as percent of recovery. Overall recovery indices are calculated, on an individual animal basis, as means of recovery indices for the individual parameters. The overall recovery index is an estimate of the general condition of the animals based on individual objective measures and is used as a numerical score for individual mice similar to the BMS score, which is based on assessment of a combination of locomotory aspects.

Tissue fixation and sectioning

Mice were anaesthetized with a 16% solution of sodium pentobarbital (Narcoren, Merial, Hallbergmoos, Germany, 5 μL/g body weight). The animals were transcardially perfused with fixative consisting of 4% formaldehyde and 0.1% $CaCl_2$ in 0.1 M cacodylate buffer, pH 7.3, for 15 min at 20 °C room temperature (RT). Following perfusion, the spinal cords were left *in situ* for 2 h at RT, after which they were dissected out and post-fixed overnight (18–22 h) at 4 °C in the solution used for perfusion. Tissue was then immersed into 15% sucrose solution in 0.1 M cacodylate buffer, pH 7.3, for 2 days at 4 °C, embedded in Tissue Tek (Sakura Finetek, Zoeterwoude, NL), and frozen by a 2-min immersion into 2-methyl-butane (isopentane) precooled to −80 °C. Serial longitudinal sections were cut in a cryostat (Leica CM3050; Leica Instruments, Nußloch, Germany). Sections, 25-μm-thick, were collected on SuperFrost Plus glass slides (Carl Roth, Karlsruhe, Germany). Sampling of sections was always performed in a standard sequence, with six sections 250 μm apart being present on each slide.

Immunohistochemistry

Procedures for immunohistochemistry have been described (Jakovcevski *et al.*, 2007). In brief, water-bath antigen de-masking was performed in 0.01 M sodium citrate solution, pH 9.0, for 30 min at 80 °C for all antigens. Non-specific binding was blocked using 5% normal serum from the species, in which the secondary antibody was produced, dissolved in phosphate buffered saline, pH 7.3 (PBS) and supplemented with 0.2% Triton X-100, 0.02% sodium azide for 1 h at RT. Incubation with the primary antibody, diluted in PBS containing 0.5% lambda-carrageenan (Sigma/Aldrich) and 0.02% sodium azide, was carried out for 3 days at 4 °C. After washing in PBS (3 × 15 min at RT), the appropriate secondary antibody diluted 1 : 200 in PBS-carrageenan solution was applied for 2 h at RT. After a subsequent wash in PBS, the sections were mounted in anti-quenching medium (RotiMount with DAPI; Carl Roth) and stored in the dark at 4 °C.

Western blot analysis

After the scratch assay in astrocyte monolayers, the culture medium was aspirated and the cells were washed with ice-cold PBS, thereafter being lysed in 100 μL of radioimmunoprecipitation assay buffer (150 mM NaCl, 50 mM Tris-HCl pH7.4, 1% NP40, 0.5% sodium deoxycholate, 1 mM sodium pyrophosphate and complete protease inhibitor cocktail (Roche)) for 30 min at 4 °C. Samples were centrifuged at 10 000 ***g*** and 4 °C for 10 min. Protein concentration was measured in the supernatants and 10 μg of protein per sample was mixed with loading buffer and heated at 95 °C for 5 min. Samples were electrophoretically separated on a 10% Tris-glycine gel and then transferred to a nitrocellulose membrane (GE Healthcare). The membrane was blocked in 4% skim milk in PBS containing 0.05% Tween 20 (PBST), incubated overnight at 4 °C with mouse anti-PSA monoclonal antibody 735 and mouse anti-GAPDH antibodies and washed three times in PBST before probing with horseradish peroxidase-conjugated secondary antibodies (Dianova) for 1 h at RT. Blots were visualized with the enhanced chemiluminescence reagent (GE Healthcare, Piscataway, NJ).

Quantifications of TH-immunoreactive axonal profiles caudal to the lesion site

Longitudinal spinal cord sections immunostained for TH were used to analyze the numbers of catecholaminergic axons in the thoracic spinal cord caudal to the lesion site at 6 weeks after spinal cord injury. All TH-positive axons projecting beyond a border 250 μm caudal to the lesion site were counted in every 5th longitudinal serial section from the spinal cord of each mouse using an Axiophot microscope (Zeiss, Oberkochen, Germany) equipped with a motorized stage and the Neurolucida software-controlled computer system (MicroBrightField, Magdeburg, Germany).

Analyses of motoneuron soma size and quantification of perisomatic terminals

Estimations of soma areas and perisomatic terminals were performed as described (Apostolova *et al.*, 2006). Longitudinal spinal cord sections immunostained for ChAT were examined under a fluorescence microscope to select sections that contained motoneuron cell bodies at a distance of approximately 250 μm caudal to the lesion scar, corresponding to the first segment of the lumbar spinal cord. Stacks of 1-μm-thick images were obtained on a LSM 510 confocal microscope (Zeiss) using a 63 × 2 oil immersion objective and digital resolution of 1024 × 1024 pixel. Six stacks were obtained consecutively in a rostro-caudal direction so that motoneurons throughout the lumbar spinal cord could be sampled. Each stack contained 3–4 motoneuronal cell bodies suitable for analysis. One image per cell at the level of the largest cell body cross-sectional area was used to measure cell body area and perimeter and to count the number of perisomatic terminals. The number of terminals was expressed as linear density per 1 mm perimeter length. Areas and perimeters were measured using ImageJ software (National Institutes of Health, Bethesda, MD). Linear density was calculated as number of counted perisomatic terminals per unit length. VGAT and VGLUT1 immunoreactive terminals around motoneuron cell bodies were counted using the same procedure. Motoneurons were identified by their size, position and ChAT immunostaining.

Estimation of expression of NF-200, GFAP and Iba-1 by immunohistochemistry

Spaced serial 25-μm-thick longitudinal spinal cord sections 250 μm apart were immunostained for NF-200, GFAP and Iba-1. To investigate the expression of NF-200 we estimated the area of the immunopositive structures normalized to the total image area using images which included the center of the lesion site. We consider this a good approximation of the overall regrowth/sprouting of the ascending and descending axons into the lesion site, which we have found to correlate well with motor recovery (Lieberoth *et al.*, 2009). To investigate the expression of GFAP and Iba-1 rostral and caudal to the lesion site we estimated the area of the immunopositive structures normalized to the total image area using ImageJ software (Papastefanaki *et al.*, 2015). This estimation was performed on images obtained on a LSM 510 confocal microscope (Zeiss) using a 40 × oil immersion objective and a digital resolution of 1024 × 1024 pixels. The confocal images were converted to gray scale to consistently adjust the threshold based on the histogram shape of the optimal color intensity. Images of the GFAP and Iba-1 immunostained areas immediately rostral and caudal to the lesion site taken from each of six longitudinal sections were analyzed per animal, and mean values from individual animals were used to calculate group mean values.

Stereological analysis

Cell counts were performed on an Axioscope microscope (Zeiss) equipped with a motorized stage and a Stereo Investigator software-controlled computer system (MicroBrightField) using the optical disector method as described (Wu *et al.*, 2012). Six longitudinal spinal cord sections 250 μm apart were used for the analysis. The sections were observed under low-power magnification (10 × objective) with a 365/420 nm excitation/emission filter set (01, Zeiss, blue fluorescence). The nuclear staining allowed for delineation of 500-μm-long spinal cord segments, 250 μm rostral and 250 μm caudal to the lesion center. The numerical density (number of cells per mm^3) of GFAP-immunoreactive cells was estimated by counting nuclei of immunolabeled cells within systematically spaced optical disectors. The parameters for this analysis were analysis: guard space depth 2 μm, base and height of the disector 3600 μm^2 and 10 μm, respectively, the distance between the disectors was 60 μm. Counting was performed using a Plan-Neofluar × 40/0.75 objective. Areas rostral and caudal to the lesion site were evaluated and, as there were no differences between them, the values were pooled and averaged per animal. The counts were performed by one observer blinded to genotypes.

Estimation of lesion scar volume

Spaced serial 25-μm-thick sections 250 μm apart were stained with cresyl violet/luxol fast blue and used for estimations of the scar volume using the Cavalieri's method of indivisibles (Apostolova *et al.*, 2006; Jakovcevski *et al.*, 2007). Areas of the scar required for volume estimation were measured directly under the optical microscope using the Neurolucida software (MicroBrightField).

Astrocyte cell culture and scratch assay

Astrocytes from brains of neonatal NCAM+/+ and NCAM−/− mice or wild-type C57BL6/J mice were prepared as described (Kleene *et al.*, 2007). Briefly, brains of neonatal NCAM+/+ and NCAM−/− mice were freed from meninges, chopped into small pieces and subjected to mechanical dissociation by successive passage through 200, 150 and 30 μm nylon mesh filters. The cells were cultured for at least 1 week at 37 °C and 5% CO_2 in DMEM supplemented with 10% fetal bovine serum on poly-L-lysine (PLL)-coated 6-well plates until they had reached confluence. Astrocytic identity of the cells was verified by immunostaining for GFAP. Twelve hours before scratch injury, the medium was changed to serum-free DMEM. The scratch injury was performed as described (Loers *et al.*, 2014). In brief, confluent astrocyte monolayers were wounded by scratching with a sterile 100 μL plastic pipette tip resulting in a cell-free cleft approximately 800 μm in width. Immediately after scratching, fresh serum-free medium and 50 μg NCAM-Fc and equimolar amounts of Fc or 5 μg EndoN were added per well. The cell-free areas were determined microscopically with a 5× objective. Time point zero indicates the maximal scratch size determined directly after the injury (100% gap size). To analyze the migration of cells into the cell-free, scratched area images of the gap were then taken 8, 24, 30 and 48 h after scratch injury using an Axiovert microscope (Carl Zeiss). Most of the astrocyte scratch assays showed cell movement from the entire gap margins. The gap width was calculated by measuring the distance between the cell bodies across the gap (perpendicular to the scratched area) using AxioVision 4.6 software (Carl Zeiss). For quantification of the gap width, a white line was placed through the cell-free area.

In vitro *proliferation of astrocytes*

After 6 days *in vitro* NCAM+/+ and NCAM−/− astrocytes were fixed with 4% formaldehyde for 30 min at RT and then washed with PBS. Blocking of non-specific immunostaining was performed for 1 h at RT with PBS containing 0.5% Triton X-100 and 1% BSA. After another wash with PBS cells were incubated overnight with antibody directed against Ki67 (1 : 500) at 4 °C. Cells were then washed three times with PBS and incubated with Cy3-labeled secondary antibody (1 : 300) for 1 h at RT, washed with PBS, and mounted in anti-fading RotiMount containing DAPI. In parallel, immunostaining for NCAM was performed to ensure that NCAM−/− astrocytes were indeed negative for NCAM. Ten images (20× magnification) from each genotype were randomly taken from two coverslips (five images per coverslip) for cell counting using an Olympus F1000 microscope (Olympus, Tokyo, Japan). Results are expressed as the percentage of Ki67 + cells of all DAPI+ cells.

Photographic documentation

Photographic documentation was performed using an Axiophot 2 microscope equipped with a digital camera AxioCam HRC and AxioVision Software (Zeiss) as well as a Leica confocal laser scanning microscope (Leica). The images were processed using ImageJ software (NIH, Bethesda, MD).

Statistical analysis

All numerical data are presented as group mean values with standard error of the mean (SEM). Student′s *t* test and two-way ANOVA with subsequent Holm–Sidak *post-hoc* tests were used for comparison as appropriate and as indicated in the figure legends. Analyses were performed using the Sigmastat v 3.5 software. The threshold value for acceptance of differences between groups was 5% ($P < 0.05$).

Results

Locomotor recovery after spinal cord injury is poorer in NCAM−/− mice compared to NCAM+/+ littermates

Locomotion of NCAM−/− mice and NCAM+/+ littermate controls was assessed by open field locomotion scoring (BMS; Basso *et al.*,

2006) and in the beam-walking test (Apostolova *et al.*, 2006) at 1, 3 and 6 weeks after injury. One week after injury, both BMS score values and foot-stepping angles indicated severe disability in both genotypes, suggesting that the severity of injury was similar in both groups. Three weeks after injury, a tendency toward worse locomotor function was observed in the NCAM−/− mice as compared to the NCAM+/+ mice. Although improvement in the quality of open field locomotion was observed in both groups 6 weeks after injury, the BMS score was by approximately 30% higher in NCAM+/+ mice as compared to NCAM−/− mice, although this difference was not statistically significant (Fig. 1a). Measurement of the foot-stepping angle also revealed reduced locomotion in NCAM−/− mice as compared to NCAM+/+ mice at both 3 and 6 weeks after injury (Fig. 1b). Similarly, the rump-height index, an estimate of the ability to support body weight during ground locomotion, also showed poorer recovery in NCAM−/− mice at 1 and 3 weeks after injury (Fig. 1c). Furthermore, the degree of gain of function (100% indicating complete recovery) for open field locomotion, foot-stepping angle and rump-height index, as calculated by the mean of these recovery indices per animal and designated as the overall recovery index, was lower at 3 and 6 weeks after injury in NCAM−/− mice than in NCAM+/+ mice (Fig. 1d).

NCAM−/− mice show increased GFAP immunoreactivity and decreased NF-200 immunoreactivity but unchanged microglial/macrophage response at the lesion site 6 weeks after injury

The effect of constitutive deletion of NCAM on survival/growth/sprouting of axons into the lesion site and on the glial response to injury was measured by analyzing the immunofluorescence intensities of neurofilament 200-positive (NF-200$^+$) axons projecting into the lesion site and astrogliosis by GFAP immunostaining at and in the vicinity of the injury site. Furthermore, immunoreactivity of Iba-1$^+$ microglia/macrophages was measured. Six weeks after spinal cord injury, the expression levels of NF-200 at and around the lesion site was lower (Fig. 2a, d and g), and the expression of GFAP was increased around the lesion site in NCAM−/− mice compared to NCAM+/+ controls (Fig. 2c, f and i). However, the expression of Iba-1 was not different between genotypes (Fig. 2b, e and h). To assess if the increased expression of GFAP in NCAM−/− animals were the consequence of increased numbers of astrocytes or upregulated GFAP expression in astrocytes, the astrocytic response was evaluated at exactly corresponding sites in sections of both genotypes by counting GFAP-immunopositive astrocytes. The numerical density (number per unit volume) of GFAP-immunopositive astrocytes was similar in NCAM+/+ vs. NCAM−/− mice ($34.2 \pm 0.67 \times 10^3$ mm^{-3} vs. $35.8 \pm 1.25 \times 10^3$ mm^{-3}, respectively, $P > 0.05$, *t* test). As the tissue response to injury includes not only astroglial scar, a GFAP-expressing area surrounding the lesion center, but also the fibrous core of the lesion scar (Chen *et al.*, 2005; Jakovcevski *et al.*, 2007), we estimated the volume of scar tissue on cresyl violet/luxol fast blue stained longitudinal spinal cord sections in NCAM+/+ and NCAM−/− mice 6 weeks after injury. The mean volume of the lesion scar in NCAM−/− and NCAM+/+ mice was similar: 1.65 ± 0.32 vs 1.77 ± 0.22 mm^3, respectively ($P > 0.05$, *t* test). Therefore, the increased GFAP expression in NCAM−/− mice was not related to higher damage susceptibility or tissue scarring.

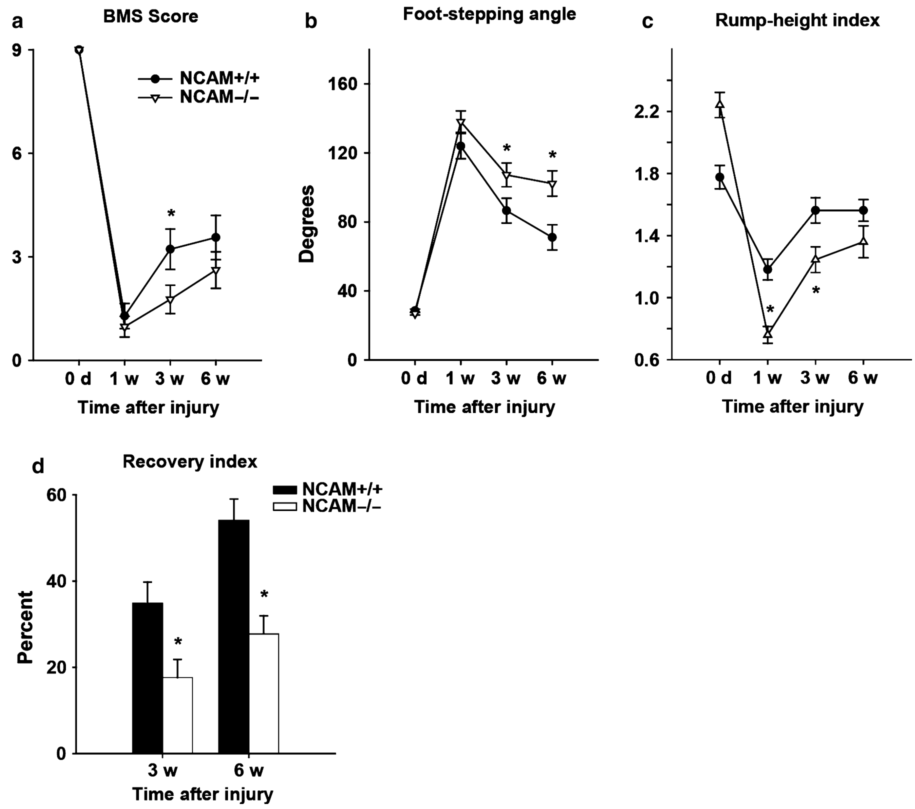

FIG. 1. Deletion of neural cell adhesion molecule (NCAM) in mice leads to poor locomotor recovery after spinal cord injury. Time course of functional recovery after compression spinal cord injury in NCAM−/− and NCAM+/+ mice. Panels a–c show mean values ± SEM as measured via the open field locomotion score (Basso Mouse Scale (BMS) score – a), foot-stepping angle (b) and rump-height index (c) before injury (day 0) and at 1, 3 and 6 weeks (w) after injury and (d) shows the overall recovery index, 3 and 6 weeks after injury. Asterisks indicate significant differences between genotypes (two-way ANOVA for repeated measurements with Holm–Sidak *post-hoc* test, $P < 0.05$; $n = 10$ mice/group).

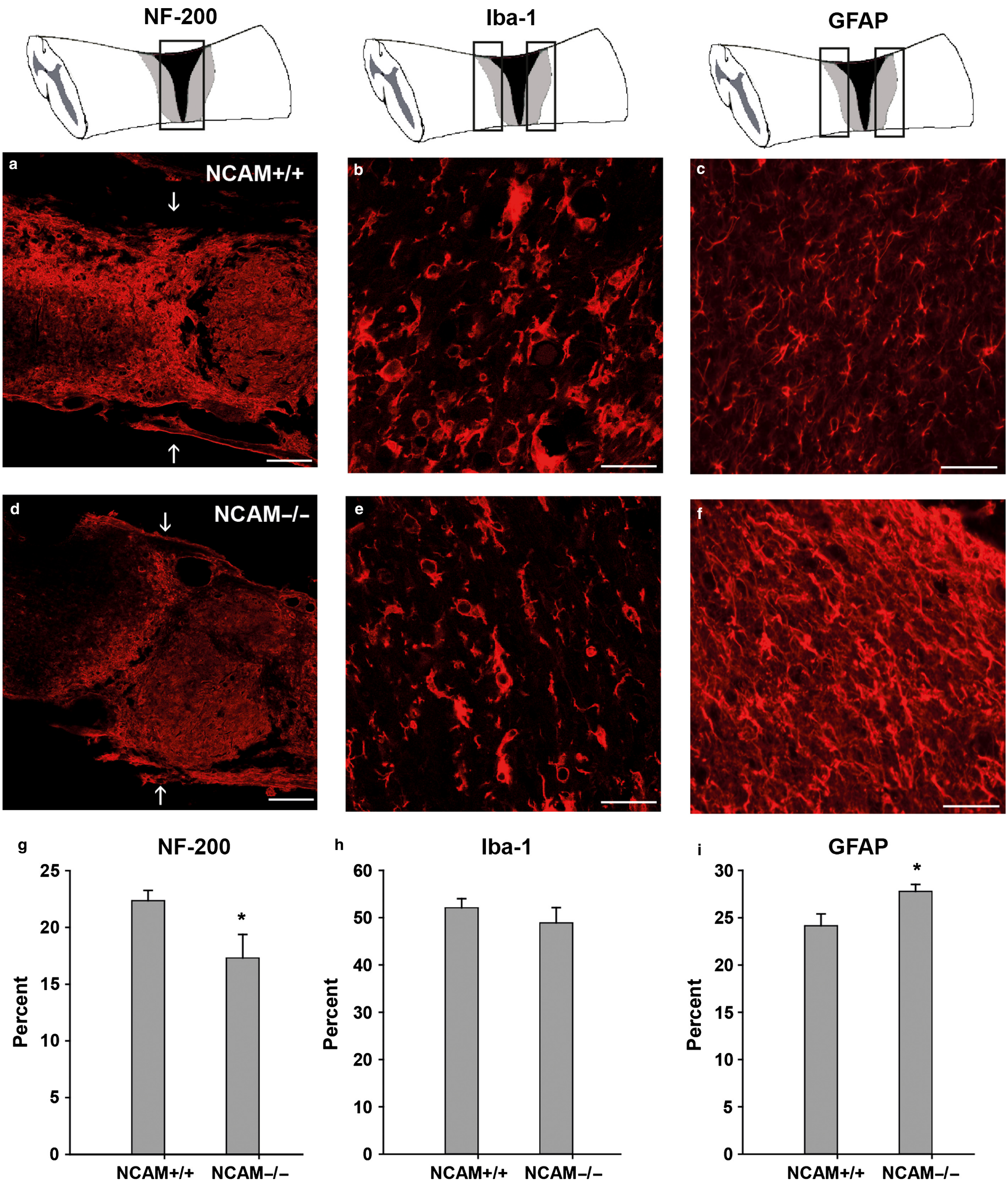

FIG. 2. Deletion of neural cell adhesion molecule (NCAM) leads to enhanced glial fibrillary acidic protein (GFAP) expression and regrowth of severed axons, but does not influence the microglial cell/macrophage response after spinal cord injury. Panels a-f show laser scanning images of staining patterns for (a, d) NF-200; (b, e) Iba-1 and (c, f) GFAP-200 in the vicinity of the lesion site in parasagittal spinal cord sections from NCAM+/+ (a–c) and NCAM–/– (d–f) mice. Arrows on panels (a) and (d) mark the lesion center. Diagrams over panels a-c depict injured spinal cords with boxed regions used for the evaluation for NF-200 (a, d), Iba-1 (b, e) and GFAP (c, f) staining. Scale bars: 50 μm (b,c,e,f) and 100 μm (a, d). (g–i) Mean values for the percent of immunostained area + SEM for NF-200 (g), Iba-1 (h) and GFAP (i) stainings. Asterisks indicate significant differences between genotypes (two-sided *t* test, $P < 0.05$; $n = 6$ mice/group).

NCAM−/− mice show decreased TH immunoreactivity below the lesion site 6 weeks after injury

Tyrosine hydroxylase-immunoreactive (TH$^+$) axons mediate catecholaminergic innervation which is important to regain locomotor function after spinal cord injury in the present injury paradigm (Jakovcevski *et al.*, 2007; Devanathan *et al.*, 2010). Therefore, numbers of TH$^+$ axons projecting beyond a border 250 μm caudal to the lesion site were counted before and at 6 weeks after injury. Before injury there was no difference between the genotypes, indicating that NCAM deletion does not influence development of these axons. After injury, however, lower numbers of TH$^+$ axonal profiles were detected in NCAM−/− mice as compared NCAM+/+ mice (Fig. 3).

NCAM−/− mice show decreased numbers of cholinergic terminals and normal numbers of glutamatergic and inhibitory terminals on cell somata of motoneurons at 6 weeks after injury

As spinal cord injury leads to severe atrophy and subsequent loss of motoneurons, we analyzed the soma size of motoneurons and their synaptic coverage approximately 500 μm caudal to the injury site. NCAM deficiency did not influence the soma size, but the linear density of cholinergic (ChAT$^+$) puncta on the soma of these neurons was reduced (Fig. 4a, b, h and g). Interestingly, the linear density of VGLUT1$^+$ and VGAT$^+$ puncta on the motoneuronal somata was not affected, indicating that NCAM ablation neither affects glutamatergic (VGLUT1$^+$) nor inhibitory (VGAT$^+$) transmitter coverage (Fig. 4c–f, i and j). As none of the measured parameters were different among genotypes in non-injured animals (Fig. 4g–j), we conclude that NCAM ablation does not influence the development of these synapses, but that the difference between genotypes reflects a specific response of young adult NCAM−/− mice to injury. Furthermore, NCAM ablation limits remodeling of cholinergic synapses on motoneurons after injury and does not affect glutamatergic or different types of inhibitory synapses.

Deletion of NCAM or application of NCAM-Fc reduce migration of cultured astrocytes

As constitutive deletion of NCAM leads to increased GFAP immunoreactivity after spinal cord injury, we asked whether NCAM would influence the migration of cultured astrocytes after scratch injury. Twenty-four hours after scratching the monolayer, the cell-free area or the gap size was reduced to approximately 57% in NCAM+/+ astrocytes (Fig. 5), whereas in NCAM−/− astrocytes the gap size was only reduced to 80% of the original gap size. Forty-eight hours after scratch injury, the gap size in monolayers of cultured NCAM+/+ astrocytes was further reduced to 34%, whereas for NCAM−/− astrocytes this reduction was only to 70% of the original gap size (Fig. 5). To analyze whether these results reflect the effect of NCAM ablation on migration or on proliferation, proliferation was measured by Ki67 immunoreactivity. In cultures of NCAM+/+ astrocytes 88.8 ± 8.8% were immunopositive and, similarly, 89.7 ± 4.9% were immunopositive in NCAM−/− astrocytes ($P > 0.05$, *t* test).

Because of the importance of PSA in different NCAM-dependent functions, including cell migration (Barral-Moran *et al.*, 2003; Lavdas *et al.*, 2006), PSA expression was tested in immunoblots, showing that in our culture system astrocytes indeed expressed PSA. We also showed that PSA was removed by EndoN application (Fig. 6a). In cultures of untreated astrocytes or astrocytes treated with Fc only, the gap size was reduced to 35% and 2.5% of the original gap size at 24 and 48 h after scratch injury, respectively (Fig. 6b). In the presence of NCAM-Fc the gap size was 52% of the original gap size after 24 h and 10% of the original size after 48 h. Application of Fc did not influence gap closure or speed of migration. Furthermore, EndoN treatment did not alter the kinetics of the gap closure. Simultaneous addition of NCAM-Fc and EndoN to the astrocyte monolayers did not influence NCAM-Fc's ability to enhance migration, indicating that the effects of NCAM on astrocyte migration were not dependent on PSA (Fig. 6b). We additionally tested if the effect of NCAM-Fc on gap closure was dependent on the endogenous expression of NCAM on astrocytes. Addition of NCAM-Fc to astrocyte cultures from NCAM−/− mice caused no difference in astrocyte gap closure compared with PLL and Fc controls (Fig. 6c). Thus, the effect of NCAM-Fc on astrocyte migration was dependent on NCAM-NCAM homophilic trans-interactions.

Discussion

Regeneration after spinal cord injury is a therapeutic challenge due to the restricted capacity of the adult mammalian central nervous

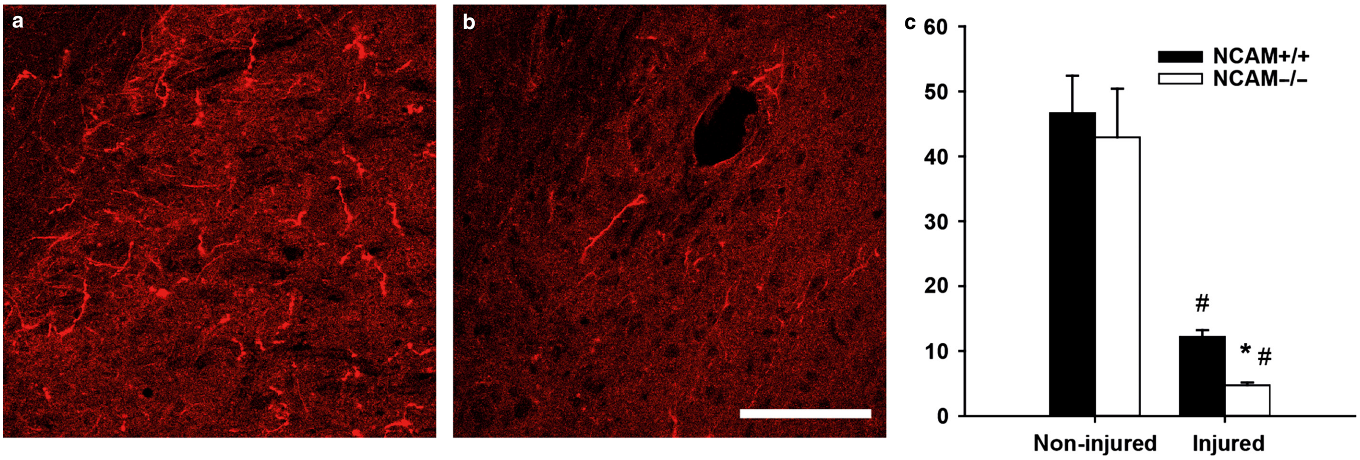

FIG. 3. Deletion of neural cell adhesion molecule (NCAM) reduces monoamiminergic reinnervation of motoneurons caudal to the lesion site. Laser scanning images of tyrosine hydroxylase immunopositive (TH$^+$) fibers in the lumbar spinal cord 6 weeks after spinal cord injury in (a) NCAM+/+ and (b) NCAM−/− mice. Scale bar: 50 μm. (c) Number of TH$^+$ axons in non-injured NCAM+/+ and NCAM−/− mice and 6 weeks after spinal cord injury. Asterisks indicate significant differences between genotypes, hatches indicate significant differences before and after injury within the genotype (two-sided *t* test, $P < 0.05$; $n = 6$ mice/group).

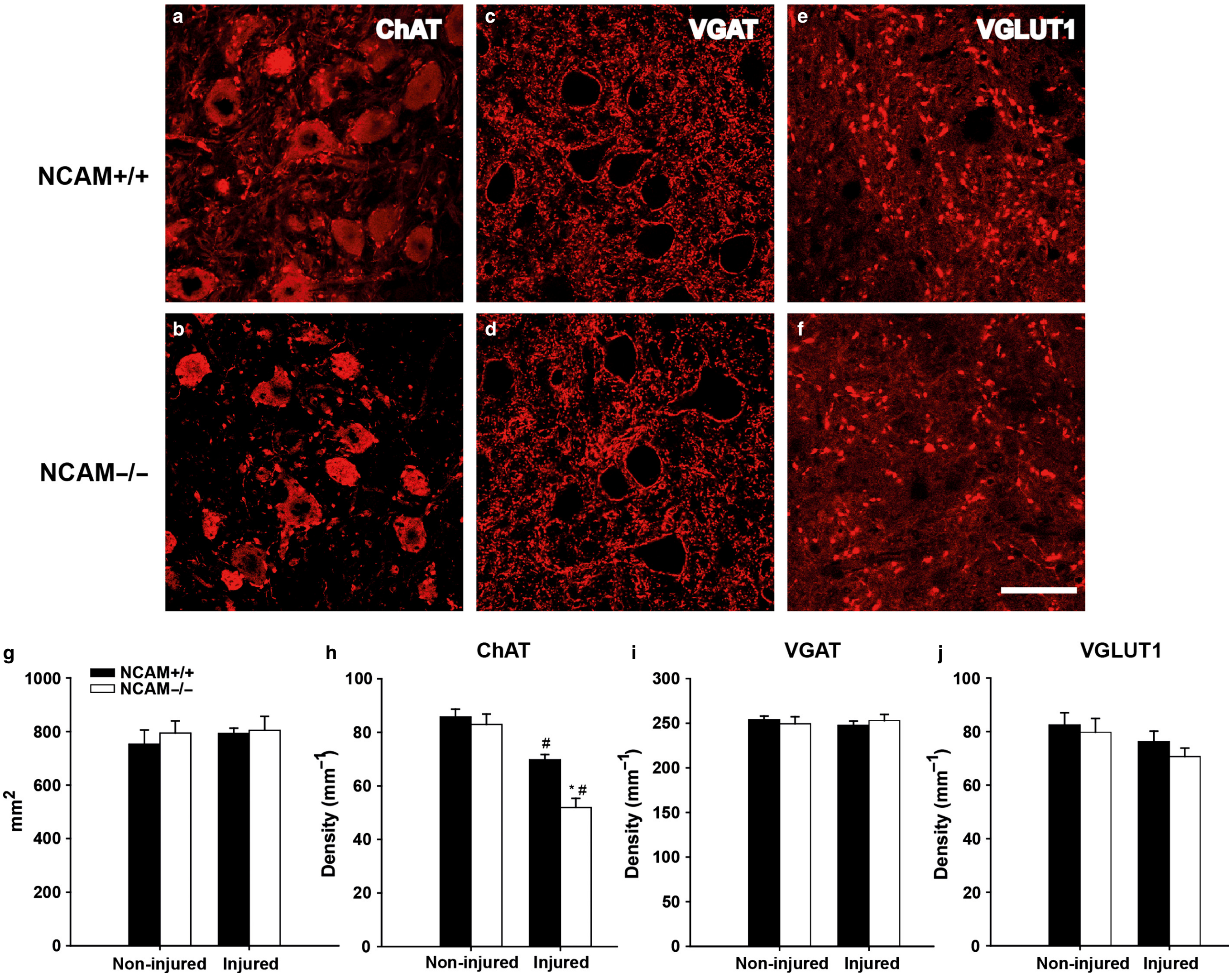

FIG. 4. Neural cell adhesion molecule (NCAM) influences the number of cholinergic immunopositive puncta around motoneurons, but does not affect inputs from inhibitory or glutamatergic synapses and cross-sectional soma area of motoneurons caudal to the lesion site. Panels a-f show laser scanning images (1 μm-thick optical sections) of (a, b) ChAT$^+$ perisomatic puncta; (c, d) VGAT$^+$ perisomatic puncta and (e, f) VGLUT$^+$ perisomatic puncta around motoneurons 250 μm caudal to the lesion site in sagittal spinal cord sections from NCAM+/+ (a, c, e) and NCAM−/− (b, d, f) mice. Scale bar: 50 μm. (g–j) Cross-sectional soma area of ChAT$^+$ neurons (g) and linear density of ChAT$^+$ puncta (h), VGAT$^+$ puncta (i) and VGLUT$^+$ puncta (j) (mean values + SEM) around motoneurons in non-injured and injured NCAM+/+ and NCAM−/− mice. Asterisks indicate significant differences between genotypes, hatches indicate significant differences before and after injury within the genotype (two-sided t test, $P < 0.05$; $n = 6$ mice/group).

system for repair (Rossignol *et al.*, 2007; Cregg *et al.*, 2014; Young, 2014). Several attempts to treat spinal cord injury in experimental rodent models focused on either improving axonal growth through the lesion site (see, for instance, Mehanna *et al.*, 2010; Ruschel *et al.*, 2015), on modulating the glial scar tissue to a more growth-permissive state (Jakovcevski *et al.*, 2007; Silver *et al.*, 2014), or on a combination of both (Hellal *et al.*, 2011; Lee *et al.*, 2012). In this study, we focused on the functions of NCAM, as it increases the interactions between neurons, neurons and astrocytes, and neurons and muscle (Rutishauser *et al.*, 1983; Keilhauer *et al.*, 1985; Acheson *et al.*, 1991; Chipman *et al.*, 2014). NCAM contributes not only to nervous system development, but also to synaptic plasticity and regeneration after injury in the adult central nervous system (Rutishauser, 2008; Hildebrandt & Dityatev, 2015). In the peripheral nervous system, impaired locomotor recovery was seen in NCAM−/− mice after sciatic nerve crush at later, but not initial phases of regeneration, a phenomenon attributed to instability of newly formed synapses in the absence of NCAM (Frey *et al.*, 2010).

In a previous study on the effects of NCAM ablation on regeneration after spinal cord contusion injury, NCAM−/− mice were impaired in locomotor recovery and axonal regrowth and apoptosis in the gray and white matter was increased, whereas activation of ERK was decreased in these mice (Zhang *et al.*, 2010). In agreement with this study, we also observed that NCAM is required, either directly or indirectly, for regeneration after spinal cord injury. In NCAM−/− mice locomotor recovery, axonal sparing/regeneration and synaptic remodeling were decreased, and glial scarring was increased compared to NCAM+/+ mice. Although the two studies were overall in good agreement, they differ with respect to the effect on astrocyte scarring, as judged by the expression of GFAP. In contrast to our study, Zhang *et al.* (2010) used the weight drop contusion model generating a more moderate lesion paradigm, whereas in our study a severe lesion was generated. It is therefore not unlikely

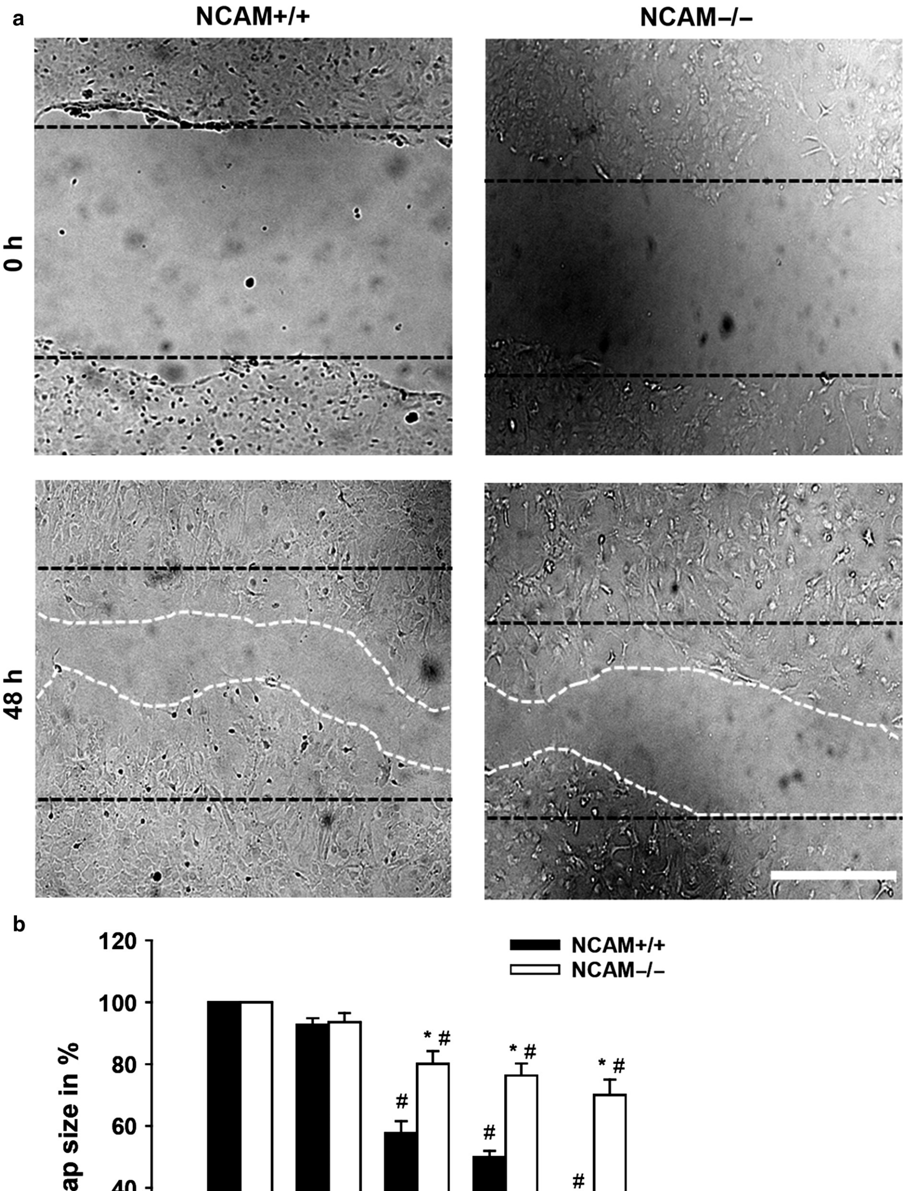

FIG. 5. Deletion of neural cell adhesion molecule (NCAM) reduces migration of astrocytes after scratch injury *in vitro*. (a) Confluent monolayers of NCAM+/+ and NCAM−/− astrocytes were scratched to form a gap. Migration of cells from into the scratched gap region was studied using an inverted phase-contrast microscope from 0 and 48 h. Scale bar = 200 μm. Black dashed line shows the initial gap size (0 h) and white dashed line shows the gap size at 48 h after the scratch. (b) Histogram showing gap width of the cell-free area in percent of the original gap size (readings at 0 h were set to 100%). Asterisks indicate significant differences between the genotypes (two-way ANOVA for repeated measurements with Holm–Sidak *post hoc* test, $P < 0.05$; $n = 6$ independent experiments). Hatches denote significant differences within the group (two-way ANOVA for repeated measurements with Holm–Sidak *post hoc* test, $P < 0.05$; $n = 6$ independent experiments).

that in the severe injury paradigm, a more pronounced change in GFAP expression levels was observed compared to the more moderate injury, thereby augmenting the effect of NCAM ablation on GFAP expression in severe spinal cord injury in our study.

Previous studies described a relationship between NCAM isoform expression and expression of the axonal isoform of neurofilament. Neurite outgrowth from human and mouse dorsal root ganglion neurons was found to be associated with enhanced expression of neurofilament proteins in conjunction with enhanced NCAM expression, suggesting a positive effect of NCAM on axons (Doherty *et al.*, 1989). These observations are in agreement with our findings that reduced NF-200 immunoreactivity by constitutive ablation of NCAM correlates with poor axonal regrowth and neuronal differentiation after injury. In this context it is noteworthy that when NCAM-mediated interactions are disrupted by treatment with a Fab fragment inhibiting NCAM function, neurofilament expression and neurite outgrowth are impeded (Keane *et al.*, 1988).

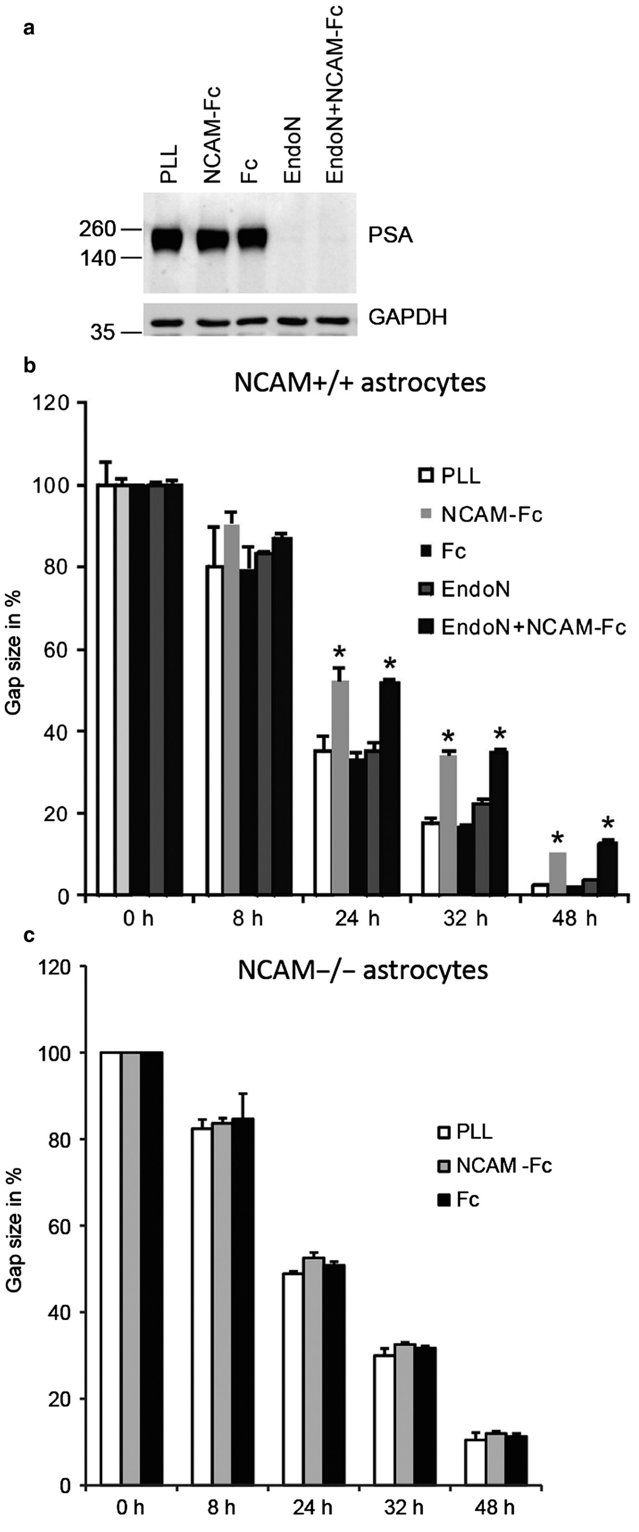

FIG. 6. Application of neural cell adhesion molecule (NCAM)-Fc reduces migration of cultured astrocytes after scratch injury. (a) Western blot analysis of PSA levels of the scratched astrocytes grown on poly-L-lysine (PLL), or treated with NCAM-Fc, Fc, EndoN or NCAM-Fc and EndoN. GAPDH is shown as loading control. (b) Confluent monolayers of NCAM+/+ astrocytes were scratched to form a gap and cells were treated with NCAM-Fc, Fc, EndoN or NCAM-Fc together with EndoN. Migration of cells into the scratch-wounded area was measured by inverted phase-contrast microscopy from 0 to 48 h (h). Histogram shows the gap width of the cell-free area in percent of the original area size (0 h was set as 100%). Asterisks indicate significant differences to the untreated cells (two-way ANOVA for repeated measurements with Holm–Sidak *post hoc* test, $P < 0.05$; $n = 3$ independent experiments). (c) Confluent monolayers of NCAM−/− astrocytes were scratched to form a gap and maintained on PLL without treatment, or with treatment with NCAM-Fc or Fc. Histogram shows the gap width of the cell-free area in percent of the original gap size (0 h was set as 100%). There were no significant differences between treatments (two-way ANOVA for repeated measurements, $P > 0.05$; $n = 2$ independent experiments).

In the context of axonal sparing/regrowth of monoaminergic pathways it is noteworthy that these modify sodium currents and firing rate in spinal motoneurons (Harvey *et al.*, 2006), and thereby contribute to controlling coordinated locomotor movements (Fouad & Pearson, 2004). By promoting re-innervation via monoaminergic pathways, plantar stepping is improved after mouse spinal cord injury (Jakovcevski *et al.*, 2007). It is likely that impaired motor functions after injury in NCAM−/− mice may be related to decreased numbers of spared/regenerated TH-immunoreactive axons originating from mesencephalic neurons which express NCAM. Notably, NCAM promotes glial cell line-derived neurotrophic factor (GDNF)-mediated survival and neurite outgrowth from dopaminergic neurons in rats (Chao *et al.*, 2002). NCAM's interaction with GDNF is also involved in promoting survival of catecholaminergic neurons (Ibáñez, 2008). Severe loss of motoneuron perisomatic terminals occurs after spinal cord injury in rats (Nacimiento *et al.*, 1995). These perisomatic ChAT immunopositive puncta form C-type synapses on motoneurons and are associated with muscarinic type 2 receptors (Davidoff & Irintchev, 1986). Activity of these synapses regulates excitability of motoneurons (Miles *et al.*, 2007) and is required for repetitive discharges of motoneurons ('central pattern generator') (Chevallier *et al.*, 2006). The fact that numbers of cholinergic synaptic terminals caudal to the injury site, which are severely reduced after injury, are further reduced in NCAM−/− mice suggests an involvement of NCAM-mediated interactions in increasing the sparing/regeneration of C-type synapses on motoneurons after injury. Similarly, numbers of septal cholinergic neurons are reduced in NCAM−/− mice, resulting in hippocampal dysplasia (Tereshchenko *et al.*, 2011). NCAM-mediated cell interactions promote choline acetyltransferase activity in embryonic chick sympathetic ganglia (Acheson & Rutishauser, 1988). NCAM also promotes formation of glutamatergic neurons during differentiation of hippocampal precursors (Shin *et al.*, 2002), but does not influence formation of GABAergic interneurons in the cerebral cortex (Pozas & Ibáñez, 2005). It is therefore not unexpected that 6 weeks after injury densities of glutamatergic and GABAergic terminals are similar in NCAM−/− and NCAM+/+ mice, suggesting that these inputs are not essential in the NCAM-dependent locomotor recovery. Furthermore, our results indicate that NCAM is not involved in preservation or regeneration of glutamatergic and GABAergic synapses on motoneurons, suggesting a finely tuned influence of NCAM on different types of synapses.

In addition to regulating synapse formation NCAM beneficially reduces directly or indirectly injury-induced reactive astrogliosis, as indicated by GFAP expression at the lesion site. As cell migration is an important feature in repair after injury, it is noteworthy that cultured astrocytes from NCAM−/− mice showed poor migration *in vitro* as compared to astrocytes from NCAM+/+ mice. However, both increased proliferation and migration of cultured astrocytes may be relevant for the *in vivo* scar formation (Jakovcevski *et al.*, 2007). Previous reports that binding of soluble immunoglobulin-like domains of NCAM to the cell surface of astrocytes (Krushel *et al.*, 1998, 1999) or addition of purified rat NCAM to rat forebrain astrocytes (Sporns *et al.*, 1995) inhibit their proliferation suggested a role for NCAM in proliferation of these cells in culture. However, our findings that proliferation of astrocytes *in vitro* was not different between genotypes and that numbers of GFAP+ astrocytes were similar in the injured spinal cords of both genotypes indicate that the expression of NCAM does not affect astrocyte proliferation after injury. Nervous system injury, axonal denervation and amyloid plaque deposition in mice activate astrocytes, as demonstrated by highly upregulated GFAP expression (Burbach *et al.*, 2004). However, in scratch-injured cultured mouse astrocytes GFAP levels were not upregulated (Puschmann *et al.*, 2010). In contrast to cultured mouse astrocytes, rat astrocytes upregulated GFAP expression after scratch injury and were more mobile than mouse astrocytes (Puschmann *et al.*, 2010). Interestingly, GFAP levels were reported to inversely correlate with astrocyte migration *in vivo* (Li *et al.*, 2010). Magnetic stimulation of spinal cord injured rats decreased lesion volume, GFAP and phosphorylated ERK expression, and increased migration of astrocytes to the lesion site (Li *et al.*, 2010). These findings indicate that GFAP expression and migration of cultured astrocytes are different *in vivo* and *in vitro*. As we did not observe any difference in number of GFAP-expressing astrocytes in the injured spinal cords between NCAM+/+ and NCAM−/− mice, we conclude that the higher GFAP levels in NCAM−/− mice are due to upregulation of astrocytic GFAP expression independent of proliferation and migration. Homophilic NCAM trans-interactions are likely the basis for our observation that NCAM-Fc reduces migration of NCAM+/+ but not NCAM−/− astrocytes *in vitro*. We propose that NCAM-Fc disrupts NCAM homophilic interactions and thereby impairs NCAM-mediated migration of astrocytes. This view is further supported by our finding that NCAM-Fc does not influence gap closure in monolayer cultures of NCAM−/− astrocytes, suggesting that heterophilic interactions of NCAM with other binding partners are not likely to play a role in migration.

As PSA is involved in NCAM-mediated oligodendroglial progenitor cell migration (Barral-Moran *et al.*, 2003) it was not expected that astrocytes migrated independently of PSA. The difference between the two studies could be due to the different cell types or culture conditions (rat O-2A progenitor cells vs. mouse astrocytes), and/or possibly also different methods of analysis. Interestingly, retrovirus-induced overexpression of PSA by mouse Schwann cells increased their migratory potential *in vitro* and *in vivo* (Lavdas *et al.*, 2006; Papastefanaki *et al.*, 2007). The combined observations indicate that PSA's role in cell migration might depend on species, cell type and developmental stage, probably due to the differential expression of PSA and PSA binding partners.

Another function of NCAM appears to come into play for regeneration after injury, as a peptide derived from NCAM's third fibronectin type III domain, representing the fibroblast growth loop, suppresses activation of microglia and production of inflammatory cytokines in aged rats (Downer *et al.*, 2010), possibly by inducing astrocytes to activate microglia (Cox *et al.*, 2013) which are relevant in central nervous system reactions to injury. Although we detected microglial cells and macrophages in both NCAM−/− and NCAM+/+ mice 6 weeks after injury, we did not observe any differences between genotypes in these cells at the lesion site between genotypes at this later stage after injury. We interpret this finding with the view that NCAM may modulate microglial cell/macrophage responses mainly during the acute, but not chronic phase of injury.

The combined observations of our study suggest that NCAM with its ability to influence neural cell interactions benefits functional recovery after spinal cord injury by enhancing axonal regrowth and reinnervation of denervated target cells, as measured for motoneurons caudal to the injury site and by reducing the size of the glial scar.

Acknowledgements

The authors are particularly grateful to Dr. Rita Gerardy-Schahn for supplying EndoN and antibody 735. We thank Eva Kronberg and Ulrike Wolters for excellent animal care, Dr. Nevena Djogo and Dr. David Lutz for help with histology, Dr. Florentia Papastefanaki for help with a graphic scheme of the spinal cord and Dr. Walid Fazeli for comments on the revised manuscript. Dr. Nevena Djogo contributed to the Western blot analysis. V. S. thanks the Council of Scientific and Industrial Research (CSIR), India, for a Senior Research Fellowship, and the German Academic Exchange Service (DAAD) for a 6-month research scholarship at the Center for Molecular Neurobiology in Hamburg. The authors declare no conflict of interest.

Abbreviations

ChAT, choline acetyltransferase; EndoN, endo-N-acyl-neuraminidase; Fc, fragment crystalline; GAPDH, glyceraldehyde-3-phosphate dehydrogenase; GFAP, glial fibrillary acidic protein; Iba-1, ionized calcium binding adaptor molecule 1; NCAM, neural cell adhesion molecule; NF, neurofilament; PSA, polysialic acid; TH, tyrosine hydroxylase; VGAT, vesicular inhibitory neurotransmitter transporter; VGluT, vesicular glutamate transporter.

References

Acheson, A. & Rutishauser, U. (1988) Neural cell adhesion molecule regulates cell contact-mediated changes in choline acetyltransferase activity of embryonic chick sympathetic neurons. *J. Cell Biol.*, **106**, 479–486.

Acheson, A., Sunshine, J.L. & Rutishauser, U. (1991) NCAM polysialic acid can regulate both cell-cell and cell-substrate interactions. *J. Cell Biol.*, **114**, 143–153.

Apostolova, I., Irintchev, A. & Schachner, M. (2006) Tenascin-R restricts posttraumatic remodeling of motoneuron innervation and functional recovery after spinal cord injury in adult mice. *J. Neurosci.*, **26**, 7849–7859.

Barral-Moran, M.J., Calaora, V., Vutskits, L., Wang, C., Zhang, H., Durbec, P., Rougon, G. & Kiss, J.Z. (2003) Oligodendrocyte progenitor migration in response to injury of glial monolayers requires the polysialic neural cell-adhesion molecule. *J. Neurosci. Res.*, **72**, 679–690.

Basso, D.M., Fisher, L.C., Anderson, A.J., Jakeman, L.B., McTigue, D.M. & Popovich, P.G. (2006) Basso Mouse Scale for locomotion detects differences in recovery after spinal cord injury in five common mouse strains. *J. Neurotraum.*, **23**, 635–659.

Bonfanti, L., Merighi, A. & Theodosis, D.T. (1996) Dorsal rhizotomy induces transient expression of the highly sialylated isoform of the neural cell adhesion molecule in neurons and astrocytes of the adult rat spinal cord. *Neuroscience*, **74**, 619–623.

Brook, G.A., Houweling, D.A., Gieling, R.G., Hermanns, T., Joosten, E.A., Bär, D.P., Gispen, W.H., Schmitt, A.B. *et al.* (2000) Attempted endogenous tissue repair following experimental spinal cord injury in the rat: involvement of cell adhesion molecules L1 and NCAM? *Eur. J. Neurosci.*, **12**, 3224–3238.

Burbach, G.J., Dehn, D., Del Turco, D., Staufenbiel, M. & Deller, T. (2004) Laser microdissection reveals regional and cellular differences in GFAP mRNA upregulation following brain injury, axonal denervation, and amyloid plaque deposition. *Glia*, **48**, 76–84.

Chao, C.C., Ma, Y.L., Chu, K.Y. & Lee, E.H. (2002) Integrin alpha and NCAM mediate the effects of GDNF on DA neuron survival, outgrowth, DA turnover and motor activity in rats. *Neurobiol. Aging*, **24**, 105–116.

Chen, S., Mantei, N., Dong, L. & Schachner, M. (1999) Prevention of neuronal cell death by neural adhesion molecules L1 and CHL1. *J. Neurobiol.*, **38**, 428–439.

Chen, J., Leong, S.Y. & Schachner, M. (2005) Differential expression of cell fate determinants in neurons and glial cells of adult mouse spinal cord after compression injury. *Eur. J. Neurosci.*, **22**, 1895–1906.

Chevallier, S., Nagy, F. & Cabelguen, J.M. (2006) Cholinergic control of excitability of spinal motoneurons in the salamander. *J. Physiol.*, **570**, 525–540.

Chipman, P.H., Schachner, M. & Rafuse, V.F. (2014) Presynaptic NCAM is required for motor neurons to functionally expand their peripheral field of innervation in partially denervated muscles. *J. Neurosci.*, **34**, 10497–10510.

Cox, F.F., Berezin, V., Bock, E. & Lynch, M.A. (2013) The neural cell adhesion molecule-derived peptide, FGL, attenuates lipopolysaccharide-induced changes in glia in a CD200-dependent manner. *Neuroscience*, **235**, 141–148.

Cregg, J.M., DePaul, M.A., Filous, A.R., Lang, B.T., Tran, A. & Silver, J. (2014) Functional regeneration beyond the glial scar. *Exp. Neurol.*, **253**, 197–207.

Cremer, H., Lange, R., Christoph, A., Plomann, M., Vopper, G., Roes, J., Brown, R., Baldwin, S. *et al.* (1994) Inactivation of the N-CAM gene in mice results in size reduction of the olfactory bulb and deficits in spatial learning. *Nature*, **367**, 455–459.

Curtis, R., Green, D., Lindsay, R.M. & Wilkin, G.P. (1993) Up-regulation of GAP-43 and growth of axons in rat spinal cord after compression injury. *J. Neurocytol.*, **22**, 51–64.

Davidoff, M.S. & Irintchev, A.P. (1986) Acetylcholinestrase activity and type C synapses in the hypoglossal, facial and spinal-cord motor nuclei of rats. An electron-microscope study. *Histochemistry*, **84**, 515–524.

Devanathan, V., Jakovcevski, I., Santuccione, A., Li, S., Lee, H.J., Peles, E., Leshchyns'ka, I., Sytnyk, V. *et al.* (2010) Cellular form of prion protein inhibits Reelin-mediated shedding of Caspr from the neuronal cell surface to potentiate Caspr-mediated inhibition of neurite outgrowth. *J. Neurosci.*, **30**, 9292–9305.

Doherty, P., Barton, C.H., Dickson, G., Seaton, P., Rowett, L.H., Moore, S.E., Gower, H.J. & Walsh, F.S. (1989) Neuronal process outgrowth of human sensory neurons on monolayers of cells transfected with cDNAs for five human N-CAM isoforms. *J. Cell Biol.*, **109**, 789–798.

Downer, E.J., Cowley, T.R., Lyons, A., Mills, K.H., Berezin, V., Bock, E. & Lynch, M.A. (2010) A novel anti-inflammatory role of NCAM-derived mimetic peptide, FGL. *Neurobiol. Aging*, **31**, 118–128.

Finne, J., Finne, U., Deagostini-Bazin, H. & Goridis, C. (1983) Occurrence of alpha 2-8 linked polysialosyl units in a neural cell adhesion molecule. *Biochem. Biophys. Res. Commun.*, **112**, 482–487.

Fouad, K. & Pearson, K. (2004) Restoring walking after spinal cord injury. *Prog. Neurobiol.*, **73**, 107–126.

Frey, A., Schachner, M. & Irintchev, A. (2010) A novel motion analysis approach reveals late recovery in C57BL/6 mice and deficits in NCAM-deficient mice after sciatic nerve crush. *J. Neurotraum.*, **27**, 815–828.

Ghosh, M., Tuesta, L.M., Puentes, R., Patel, S., Melendez, K., El Maarouf, A., Rutishauser, U. & Pearse, D.D. (2012) Extensive cell migration, axon regeneration, and improved function with polysialic acid-modified Schwann cells after spinal cord injury. *Glia*, **60**, 979–992.

Harvey, P.J., Li, X., Li, Y. & Bennett, D.J. (2006) Endogenous monoamine receptor activation is essential for enabling persistent sodium currents and repetitive firing in rat spinal motoneurons. *J. Neurophysiol.*, **96**, 1171–1186.

Hellal, F., Hurtado, A., Ruschel, J., Flynn, K.C., Laskowski, C.J., Umlauf, M., Kapitein, L.C., Strikis, D. *et al.* (2011) Microtubule stabilization reduces scarring and causes axon regeneration after spinal cord injury. *Science*, **331**, 928–931.

Hildebrandt, H. & Dityatev, A. (2015) Polysialic acid in brain development and synaptic plasticity. *Top. Curr. Chem.*, **366**, 55–96.

Ibáñez, C.F. (2008) Catecholaminergic neuron survival: getting hooked on GDNF. *Nat. Neurosci.*, **11**, 735–736.

Jakovcevski, I., Wu, J., Karl, N., Leshchyns'ka, I., Sytnyk, V., Chen, J., Irintchev, A. & Schachner, M. (2007) Glial scar expression of CHL1, the close homolog of the adhesion molecule L1, limits recovery after spinal cord injury. *J. Neurosci.*, **27**, 7222–7233.

Joosten, E.A. & Bär, D.P. (1999) Axon guidance of outgrowing corticospinal fibres in the rat. *J. Anat.*, **194**, 15–32.

Kadmon, G., Kowitz, A., Altevogt, P. & Schachner, M. (1990) The neural cell adhesion molecule N-CAM enhances L1-dependent cell-cell interactions. *J. Cell Biol.*, **110**, 193–208.

Karimi-Abdolrezaee, S. & Billakanti, R. (2012) Reactive astrogliosis after spinal cord injury-beneficial and detrimental effects. *Mol. Neurobiol.*, **46**, 251–264.

Keane, R.W., Mehta, P.P., Rose, B., Honig, L.S., Loewenstein, W.R. & Rutishauser, U. (1988) Neural differentiation, NCAM-mediated adhesion, and gap junctional communication in neuroectoderm. A study in vitro. *J. Cell Biol.*, **106**, 1307–1319.

Keilhauer, G., Faissner, A. & Schachner, M. (1985) Differential inhibition of neurone-neurone, neurone-astrocyte, and astrocyte-astrocyte adhesion by L1, L2 and N-CAM antibodies. *Nature*, **316**, 728–730.

Kiss, J.Z., Troncoso, E., Djebbara, Z., Vutskits, L. & Muller, D. (2001) The role of neural cell adhesion molecules in plasticity and repair. *Brain Res. Brain Res. Rev.*, **36**, 175–184.

Kleene, R., Loers, G., Langer, J., Frobert, Y., Buck, F. & Schachner, M. (2007) Prion protein regulates glutamate-dependent lactate transport of astrocytes. *J. Neurosci.*, **27**, 12331–12340.

Kristiansen, L.V., Marques, F.A., Soroka, V., Ronn, L.C., Kiselyov, V., Pedersen, N., Berezin, V. & Bock, E. (1999) Homophilic NCAM interactions interfere with L1 stimulated neurite outgrowth. *FEBS Lett.*, **24**, 30–34.

Krushel, L.A., Tai, M.H., Cunningham, B.A., Edelman, G.M. & Crossin, K.L. (1998) Neural cell adhesion molecule (N-CAM) domains and intracellular signaling pathways involved in the inhibition of astrocyte proliferation. *Proc. Natl. Acad. Sci. USA*, **95**, 2592–2596.

Krushel, L.A., Cunningham, B.A., Edelman, G.M. & Crossin, K.L. (1999) NF-kappaB activity is induced by neural cell adhesion molecule binding to neurons and astrocytes. *J. Biol. Chem.*, **274**, 2432–2439.

Kumar, S., Prakash, J., Kataria, H. & Kaur, G. (2012) Enzymatic removal of polysialic acid from neural cell adhesion molecule interrupts gonadotropin releasing hormone (GnRH) neuron-glial remodeling. *Mol. Cell. Endocrinol.*, **348**, 95–103.

Lavdas, A.A., Franceschini, I., Dubois-Dalcq, M. & Matsas, R. (2006) Schwann cells genetically engineered to express PSA show enhanced migratory potential without impairment of their myelinating ability in vitro. *Glia*, **53**, 868–878.

Lee, H.J., Bian, S., Jakovcevski, I., Wu, B., Irintchev, A. & Schachner, M. (2012) Delayed applications of L1 and chondroitinase ABC promote recovery after spinal cord injury. *J. Neurotraum.*, **29**, 1850–1863.

Li, Z., Fang, Z.Y., Xiong, L. & Huang, X.L. (2010) Spinal cord injury-induced astrocyte migration and glial scar formation: effects of magnetic stimulation frequency. *Indian J. Biochem. Bio.*, **47**, 359–363.

Lieberoth, A., Splittstoesser, F., Katagihallimath, N., Jakovcevski, I., Loers, G., Ranscht, B., Karagogeos, D., Schachner, M. *et al.* (2009) Lewis(x) and alpha2,3-sialyl glycans and their receptors TAG-1, Contactin, and L1 mediate CD24-dependent neurite outgrowth. *J. Neurosci.*, **29**, 6677–6690.

Loers, G. & Schachner, M. (2007) Recognition molecules and neural repair. *J. Neurochem.*, **101**, 865–882.

Loers, G., Saini, V., Mishra, B., Papastefanaki, F., Lutz, D., Chaudhury, S., Ripoll, D.R., Wallqvist, A. *et al.* (2014) Nonyloxytryptamine mimics polysialic acid and modulates neuronal and glial functions in cell culture. *J. Neurochem.*, **128**, 88–100.

Maness, P.F. & Schachner, M. (2007) Neural recognition molecules of the immunoglobulin superfamily: signaling transducers of axon guidance and neuronal migration. *Nat. Neurosci.*, **10**, 19–26.

Mehanna, A., Jakovcevski, I., Acar, A., Xiao, M., Loers, G., Rougon, G., Irintchev, A. & Schachner, M. (2010) Polysialic acid glycomimetic promotes functional recovery and plasticity after spinal cord injury in mice. *Mol. Ther.*, **18**, 34–43.

Miles, G.B., Hartley, R., Todd, A.J. & Brownstone, R.M. (2007) Spinal cholinergic interneurons regulate the excitability of motoneurons during locomotion. *Proc. Natl. Acad. Sci. USA*, **104**, 2448–2453.

Nacimiento, W., Sappok, T., Brook, G.A., Tóth, L., Schoen, S.W., Noth, J. & Kreutzberg, G.W. (1995) Stuctural changes of anterior horn neurons and their synaptic input caudal to low thoracic spinal cord hemisection in the adult rat: a light and electron microscopic study. *Acta Neuropathol.*, **90**, 552–564.

Papastefanaki, F., Chen, J., Lavdas, A.A., Thomaidou, D., Schachner, M. & Matsas, R. (2007) Grafts of Schwann cells engineered to express PSA-NCAM promote functional recovery after spinal cord injury. *Brain*, **130**, 2159–2174.

Papastefanaki, F., Jakovcevski, I., Poulia, N., Djogo, N., Schulz, F., Martinovic, T., Ciric, D., Loers, G. *et al.* (2015) Intraspinal delivery of polyethylene glycol-coated gold nanoparticles promotes recovery after spinal cord injury. *Mol. Ther.*, **23**, 993–1002.

Pozas, E. & Ibáñez, C.F. (2005) GDNF and GFRalpha1 promote differentiation and tangential migration of cortical GABAergic neurons. *Neuron*, **45**, 701–713.

Puschmann, T.B., Dixon, K.J. & Turnley, A.M. (2010) Species differences in reactivity of mouse and rat astrocytes in vitro. *Neurosignals*, **18**, 152–163.

Rossignol, S., Schwab, M., Schwartz, M. & Fehlings, M.G. (2007) Spinal cord injury: time to move? *J. Neurosci.*, **27**, 11782–11792.

Ruschel, J., Hellal, F., Flynn, K.C., Dupraz, S., Elliott, D.A., Tedeschi, A., Bates, M., Sliwinski, C. *et al.* (2015) Axonal regeneration. Systemic administration of epothilone B promotes axon regeneration after spinal cord injury. *Science*, **348**, 347–352.

Rutishauser, U. (2008) Polysialic acid in the plasticity of the developing and adult vertebrate nervous system. *Nat. Rev. Neurosci.*, **9**, 26–35.

Rutishauser, U., Grumet, M. & Edelman, G.M. (1983) Neural cell adhesion molecule mediates initial interactions between spinal cord neurons and muscle cells in culture. *J. Cell Biol.*, **97**, 145–152.

Schachner, M. (1997) Neural recognition molecules and synaptic plasticity. *Curr. Opin. Cell Biol.*, **9**, 627–634.

Senkov, O., Sun, M., Weinhold, B., Gerardy-Schahn, R., Schachner, M. & Dityatev, A. (2006) Polysialylated neural cell adhesion molecule is involved in induction of long-term potentiation and memory acquisition and consolidation in a fear-conditioning paradigm. *J. Neurosci.*, **26**, 10888–10898.

Senkov, O., Tikhobrazova, O. & Dityatev, A. (2012) PSA-NCAM: synaptic functions mediated by its interactions with proteoglycans and glutamate receptors. *Int. J. Biochem. Cell Biol.*, **44**, 591–595.

Shin, M.H., Lee, E.G., Lee, S.H., Lee, Y.S. & Son, H. (2002) Neural cell adhesion molecule (NCAM) promotes the differentiation of hippocampal precursor cells to a neuronal lineage, especially to a glutamatergic neural cell type. *Exp. Mol. Med.*, **34**, 401–410.

Silver, J. & Miller, J.H. (2004) Regeneration beyond glial scar. *Nat. Rev. Neurosci.*, **5**, 146–156.

Silver, J., Schwab, M.E. & Popovich, P.G. (2014) Central nervous system regenerative failure: role of oligodendrocytes, astrocytes, and microglia. *Cold Spring Harbor. Perspect Biol.*, **7**, a020602.

Sporns, O., Edelman, G.M. & Crossin, K.L. (1995) The neural cell adhesion molecule (N-CAM) inhibits proliferation in primary cultures of rat astrocytes. *Proc. Natl. Acad. Sci. USA*, **92**, 542–546.

Takei, K., Chan, T.A., Wang, F.S., Deng, H., Rutishauser, U. & Jay, D.G. (1999) The neural cell adhesion molecules L1 and NCAM-180 act in different steps of neurite outgrowth. *J. Neurosci.*, **19**, 9469–9479.

Tereshchenko, Y., Morellini, F., Dityatev, A., Schachner, M. & Irintchev, A. (2011) Neural cell adhesion molecule ablation in mice causes hippocampal dysplasia and loss of septal cholinergic neurons. *J. Comp. Neurol.*, **519**, 2475–2492.

Tzeng, S.F., Cheng, H., Lee, Y.S., Wu, J.P., Hoffer, B.J. & Kuo, J.S. (2001) Expression of neural cell adhesion molecule in spinal cords following complete transection. *Life Sci.*, **68**, 1005–1012.

Wu, B., Matic, D., Djogo, N., Szpotowicz, E., Schachner, M. & Jakovcevski, I. (2012) Improved regeneration after spinal cord injury in mice lacking functional T- and B-lymphocytes. *Exp. Neurol.*, **237**, 274–285.

Young, W. (2014) Spinal cord regeneration. *Cell Transplant.*, **23**, 573–611.

Zhang, Y., Zhang, X., Wu, D., Verhaagen, J., Richardson, P.M., Yeh, J. & Bo, X. (2007) Lentiviral-mediated expression of polysialic acid in spinal cord and conditioning lesion promote regeneration of sensory axons into spinal cord. *Mol. Ther.*, **15**, 1796–1804.

Zhang, S., Xia, Y.Y., Lim, H.C., Tang, F.R. & Feng, Z.W. (2010) NCAM-mediated locomotor recovery from spinal cord contusion injury involves neuroprotection, axon regeneration and synaptogenesis. *Neurochem. Int.*, **56**, 919–929.